

- [4] S. B. Worm and R. Pregla, "Hybrid mode analysis of arbitrarily shaped planar microwave structures by the method of lines," *IEEE Trans. Microwave Theory Tech.*, vol. MTT-32, pp. 191-196, 1984.
- [5] Z. Q. Chen and B. X. Gao, "Deterministic approach to full-wave analysis of discontinuities in MIC's using the method of lines," *IEEE Trans. Microwave Theory Tech.*, vol. 37, pp. 606-611, Mar. 1989.
- [6] R. H. Jansen, "The spectral domain approach for microwave integrated circuits," *IEEE Trans. Microwave Theory Tech.*, vol. MTT-33, pp. 1043-1056, Oct. 1985.
- [7] S. B. Worm, "Analysis of planar microwave structures with arbitrary contour" (in German), Ph.D. thesis, Fern Univ., Hagen, Federal Republic of Germany, 1983.
- [8] W. Pascher and R. Pregla, "Full wave analysis of complex planar microwave structures," *Radio Sci.*, vol. 22, pp. 999-1002, 1987.
- [9] W. Pascher, "Full wave analysis of complex discontinuities in multilayered planar waveguides by the method of lines," in preparation.
- [10] H. Diestel and S. B. Worm, "Analysis of hybrid field problems by the method of lines with nonequidistant discretization," *IEEE Trans. Microwave Theory Tech.*, vol. MTT-32, pp. 633-638, June 1984.
- [11] U. Schulz and R. Pregla, "A new technique for the analysis of the dispersion characteristics of planar waveguides," *Arch. Elek. Übertragungs.*, vol. 34, pp. 169-173, 1980.
- [12] L. P. Schmidt, "Rigorous computation of the frequency dependent properties of filters and coupled resonators composed from transverse microstrip discontinuities," in *Proc. 10th European Microwave Conf.*, (Warsaw) 1980, pp. 436-440.
- [13] N. H. L. Koster and R. H. Jansen, "The microstrip step discontinuity: A revised description," *IEEE Trans. Microwave Theory Tech.*, vol. MTT-34, pp. 213-223, 1986.
- [14] G. Kompa, "The frequency dependent transmission properties of stripline step discontinuities, filters, and stubs in microstrip technique" (in German), Ph.D. thesis, RWTH Aachen, Federal Republic of Germany, 1975.

Arbitrary Pulse Shape Synthesis via Nonuniform Transmission Lines

SCOTT C. BURKHART, MEMBER, IEEE, AND RUSSELL B. WILCOX

Abstract—A discrete inverse scattering technique is used to define the impedance profile for a nonuniform transmission line which reflects an arbitrary waveform. Initially charged nonuniform lines, switched out into a general load, can also be synthesized by this method and are discussed. The direct or "layer peeling" algorithm is applied to generate profiles which were subsequently analyzed using the one-dimensional finite difference method and fabricated in stripline. Excitation for the nonuniform line was done using a charged line connected to a photoconductive silicon switch triggered by a mode locked YLF laser. Several lines were fabricated relevant to amplitude modulation of the master oscillator laser pulse for fusion experiments.

I. INTRODUCTION

Nonuniform impedance transmission lines have been studied by various researchers for the past four decades. An early entrant in this area was Orlov [1], who first developed the theory for nonuniform lines of arbitrary impedance profile. His work was taken further by Youla [2] and Wohlers [3], who developed realizability and uniqueness proofs for resistive or inductive terminations in the frequency domain. Gopinath [4] presented an excellent treatise on the existence and uniqueness of nonuniform transmission lines in the time domain given the impulse response. His uniqueness constraint was that the transmission line propagation velocity be constant. Given Gopinath's result,

Manuscript received November 6, 1989; revised April 30, 1990. This work was performed under the auspices of the U.S. Department of Energy by the Lawrence Livermore National Laboratory under Contract W-7405-ENG-48.

The authors are with the Lawrence Livermore National Laboratory, P.O. Box 808, Livermore, CA 94550.
IEEE Log Number 9037691.

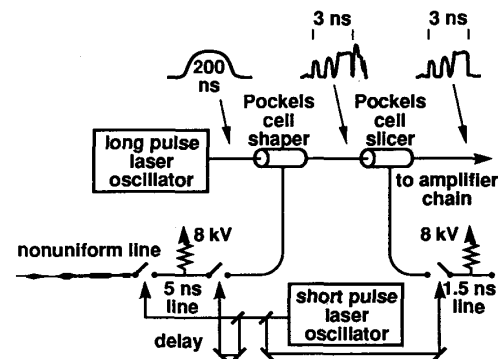


Fig. 1. Schematic of the optical pulse shaping apparatus used in the Livermore laser fusion facility. A square 4 kV wave is reflected and shaped by the nonuniform transmission line and then routed to the Pockels cell. The shaped optical pulse is windowed in time by the "slicer" Pockels cell, which improves the contrast while also slicing away unwanted residuals.

what was subsequently needed was a practical inversion or synthesis technique, and this was provided by Bruckstein and Kailath in their two landmark papers [5], [6]. This method is reviewed and extended here to include switched charged lines and is then applied to a particular pulse shaping problem relevant to laser fusion experiments.

A review of recent pulse shaping methods for pulses less than 10 ns in length primarily involves shorted stubs and delay lines of different lengths which are recombined to synthesize discrete stepped waveforms. The original paper on this was by Ross [7], who generated 1-3 GHz wave packets from a step input using shorted and open stubs along a delay line. The same method was applied by Luthjens *et al.* [8], [9] to generate nanosecond square waves and by Margulis and Persson [10], who developed a semirigid coaxial cable version capable of sub-100-ps shaping. Haner and Warren [12] demonstrated picosecond low-voltage shaping by combining identically shaped, programmable amplitude pulses, each delayed so as to build up the desired envelope.

Precision optical pulse shaping is a requirement for efficient laser drive of inertial confinement fusion targets. This is a result of target physics constraints as well as of system nonlinearities and laser saturation. The optical pulse shaping apparatus we used is shown in Fig. 1, where the shaped electrical pulse is generated by an Auston switch [13] and a nonuniform line. Until recently, the nonuniform line used was a conductive strip suspended within a conducting U-shaped channel by a series of adjustable dielectric micrometer extensions [14]-[16]. However, hysteresis, tedious trial and error adjustment, and an inability to make pulses required for some recent experiments have limited its usefulness. Applying the methods derived in the following section, stripline nonuniform lines have been synthesized which generate our required pulse shapes.

II. LAYER PEELING TRANSMISSION LINE SYNTHESIS

Consider the nonuniform line shown in Fig. 2, represented by a series of $N + 1$ uniform impedance sections of equal electrical length. Each section is characterized by its impedance $Z(x)$, current $I(x, t)$, and voltage $V(x, t)$. To carry out the synthesis it is convenient to transform the voltage and current into right-

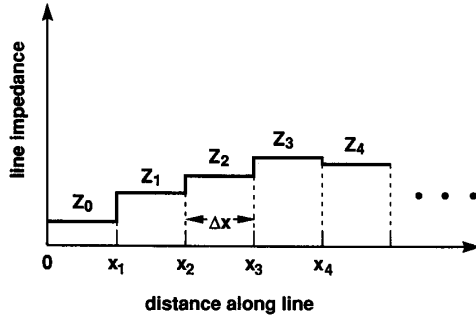


Fig. 2. The nonuniform transmission line is discretized into equal-length sections of constant impedance. The propagation velocity is assumed to be a constant independent of x .

and left-traveling waves:

$$WR(x, t) = (V(x, t)/\sqrt{Z(x)} + I(x, t)\sqrt{Z(x)})/2 \quad (1)$$

$$WL(x, t) = (V(x, t)/\sqrt{Z(x)} - I(x, t)\sqrt{Z(x)})/2. \quad (2)$$

At each junction the waves are designated as shown in Fig. 3, WR_i^- being the right-traveling wave amplitude at location $x_i - \epsilon$, and WR_i^+ the right-traveling wave amplitude at $x_i + \epsilon$, where $\epsilon \rightarrow 0$. The left-traveling waves WL_i^- and WL_i^+ are similarly defined.

From continuity of voltage and current at $x = x_i$ we have

$$\sqrt{Z_{i-1}}(WR_i^- + WL_i^-) = \sqrt{Z_i}(WR_i^+ + WL_i^+) \quad (3)$$

$$\frac{1}{\sqrt{Z_{i-1}}}(WR_i^- - WL_i^-) = \frac{1}{\sqrt{Z_i}}(WR_i^+ - WL_i^+). \quad (4)$$

Defining the reflection coefficient

$$k_i = \frac{Z_i - Z_{i-1}}{Z_i + Z_{i-1}} \quad (5)$$

we solve for the wave variables WR_i^+ and WL_i^+ :

$$\begin{pmatrix} WR_i^+ \\ WL_i^+ \end{pmatrix} = (1 - k_i^2)^{-1/2} \begin{pmatrix} 1 & -k_i \\ -k_i & 1 \end{pmatrix} \begin{pmatrix} WR_i^- \\ WL_i^- \end{pmatrix}. \quad (6)$$

Equation (6) is written in transfer matrix form, which is suitable for the layer peeling synthesis. Now, let the given right- and left-traveling waves (incident and reflected waves) at $x = x_1$ be defined as the piecewise-constant functions

$$\begin{aligned} WR_1^- &= a_1 & 0 \leq t < 2\Delta t \\ & a_2 & 2\Delta t \leq t < 4\Delta t \\ & a_3 & 4\Delta t \leq t < 6\Delta t \\ & \vdots & \\ & a_N & 2(N-1)\Delta t \leq t < 2N\Delta t \end{aligned} \quad (7)$$

$$\begin{aligned} WL_1^- &= b_1 & 0 \leq t < 2\Delta t \\ & b_2 & 2\Delta t \leq t < 4\Delta t \\ & b_3 & 4\Delta t \leq t < 6\Delta t \\ & \vdots & \\ & b_N & 2(N-1)\Delta t \leq t < 2N\Delta t \end{aligned} \quad (8)$$

where $\Delta t = \Delta x/c$, c being the wave propagation velocity. At time $t = 0$, the transmission line has an initial charge voltage V_0 ,

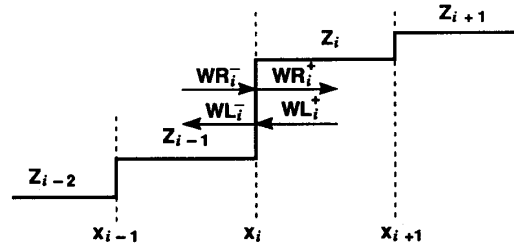


Fig. 3. Notation used to designate the right- and left-traveling waves. The subscript denotes the junction, and the superscript + or - refers to the side of the junction on which the wave amplitudes are measured.

which is equivalent to a standing zero-frequency wave:

$$WR_i^+(t=0) = WL_i^+(t=0) = \frac{V_0}{2\sqrt{Z_i}}, \quad i = 1, 2, 3, \dots, N. \quad (9)$$

Finally, we adopt a notation which samples the section mid-points of the two waveforms and follows the right-traveling wave in time:

$$WL_{i,j}^- \equiv WL(x = i\Delta x - \epsilon, t = (i+2(j-1))\Delta t) \quad (10a)$$

$$WL_{i,j}^+ \equiv WL(x = i\Delta x + \epsilon, t = (i+2(j-1))\Delta t) \quad (10b)$$

$$WR_{i,j}^- \equiv WR(x = i\Delta x - \epsilon, t = (i+2(j-1))\Delta t) \quad (10c)$$

$$WR_{i,j}^+ \equiv WR(x = i\Delta x + \epsilon, t = (i+2(j-1))\Delta t) \quad (10d)$$

$$\epsilon \rightarrow 0.$$

With this notation, we write the following from (7), (8), and (9), with the additional constraint that the impedance connected to the last line section at $x = x_N + \Delta x$ is infinity (open circuit). This allows us to write (13), extending the initial condition (9) until the right-traveling wave reaches the section Z_i . The constraint is not necessary for $V_0 = 0$:

$$WR_{i,j}^- = a_j, \quad j = 1, 2, 3, \dots, N \quad (11)$$

$$WL_{i,j}^- = b_j, \quad j = 1, 2, 3, \dots, N \quad (12)$$

$$WL_{i,1}^+ = \frac{V_0}{2\sqrt{Z_i}}. \quad (13)$$

A key point of the formulation thus far is that the transmission line has been broken into sections of electrical length Δt , while the excitation and response functions are discretized into sections of length $2\Delta t$. This is because a change in the reflected wave caused by the junction $i+1$ occurs no sooner than $2\Delta t$ after that due to junction i .

Equation (6) is now rewritten to explicitly include the time index:

$$\begin{pmatrix} WR_{i,j}^+ \\ WL_{i,j}^+ \end{pmatrix} = (1 - k_i^2)^{-1/2} \begin{pmatrix} 1 & -k_i \\ -k_i & 1 \end{pmatrix} \begin{pmatrix} WR_{i,j}^- \\ WL_{i,j}^- \end{pmatrix}. \quad (14)$$

Equation (14) can be solved for k_i when $j=1$ using the initial condition (13):

$$WL_{i,1}^+ = \frac{V_0}{2\sqrt{Z_i}} = (1 - k_i^2)^{-1/2} (-k_i WR_{i,1}^- + WL_{i,1}^-). \quad (15)$$

Applying (5) to eliminate Z_i , and rearranging,

$$k_i = \frac{WL_{i,1}^- - \frac{V_0}{2\sqrt{Z_{i-1}}}}{WR_{i,1}^- - \frac{V_0}{2\sqrt{Z_{i-1}}}}. \quad (16)$$

With (16) we peel away one layer of the piecewise-constant impedance transmission line and obtain the value for Z_i using (5). Equation (14) is then applied to determine the values for $WR_{i,j}^+$ and $WL_{i,j}^+$. At this point we have derived the equations such that, given the initial charge V_0 and the right- and left-traveling waves to the left of any junction i , we can calculate the right- and left-traveling waves to the right of the junction. What remains is to relate the waves at junction i to those at junction $i+1$. This is trivially done, since the translation by Δx along any of the Z_i sections corresponds to a time shift of $\pm \Delta t$ for the right ($-\Delta t$) and left ($+\Delta t$) traveling waves. Using the indexing from (10), we translate by Δx and advance time by Δt :

$$WR_{i+1,j}^- = WR_{i,j}^+, \quad j=1,2,3,\dots,N-i \quad (17a)$$

$$WL_{i+1,j}^- = WL_{i,j+1}^+, \quad j=1,2,3,\dots,N-i. \quad (17b)$$

This completes the derivation, since one layer has been peeled away and a translation to the next junction has been done. The entire process is summarized in the following algorithm:

a) Start with a given Z_0 , $i=1$, and with

$$WR_{1,j}^- = a_j, \quad j=1,2,3,\dots,N \quad (\text{from (7)})$$

$$WL_{1,j}^- = b_j, \quad j=1,2,3,\dots,N \quad (\text{from (8)}).$$

b) Solve for k_i from (16) and then solve for Z_i using (5).

c) Calculate $WR_{i,j}^+$ and $WL_{i,j}^+$ using k_i from step (b), and by applying (14) for $j=1,2,3,\dots,N+1-i$.

d) Calculate $WR_{i+1,j}^-$ and $WL_{i+1,j}^-$ using (17).

e) Increment i by 1, and repeat steps (b) through (e) until $i=N$.

The three cases of initial and boundary conditions for which this algorithm is useful are

- i) $V_0=0$, $a_j \neq 0$: Initially discharged line which modifies and reflects the incident wave.
- ii) $V_0 \neq 0$, $a_j=0$ for all j : Initially charged line which is switched into the pure resistive matched load Z_0 .
- iii) $V_0 \neq 0$, $a_j \neq 0$: Initially charged line which is switched into an arbitrary load. In this case the a_j are calculated from the b_j and from the load reflected wave response.

Case (i) is applied in the following example.

III. COMPUTATIONAL ASPECTS

The simplicity of the layer peeling algorithm is complicated somewhat by the reflected wave amplitude, bandwidth, and, for case (i) above, the incident wave a_j . The amplitude was easiest to handle, since we were seeking a specific reflected wave shape irrespective of its peak amplitude. During step (b) in the synthesis algorithm, a value of Z_i may fail to satisfy $Z_{\min} \leq Z_i \leq Z_{\max}$, where (Z_{\min}, Z_{\max}) is the physically realizable impedance range. When this happens, one can simply scale down the desired wave (b_j) by some factor, scale up V_0 , or scale up the incident wave (a_j) and start over at step (a). Note that the reflected wave (b_j) should be scaled with an offset of $V_0(R_{\text{load}}/(Z_0 + R_{\text{load}}))$, where R_{load} is the resistive part of the load impedance. Thus for (i), the b_j are scaled with no offset, while for (ii) the b_j are scaled and then offset by $V_0/2$.

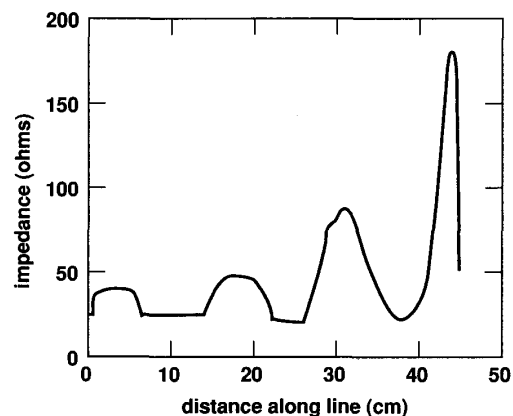


Fig. 4. Transmission line impedance profile generated by the layer peeling method. The incident waveform was a unit step, and the reflected waveform is that of Fig. 7.

The bandwidth of the reflected wave can be a problem in case (i) above, since the reflected wave power spectrum cannot exceed that of the incident wave at any frequency. We dealt with this by filtering both waveforms with a fourth-order Bessel low-pass filter, where the 3 dB point was chosen to modify the waveforms by a small but acceptable amount. Bandwidth problems are observed when excessive scaling is required to achieve a solution.

For case (i), the first element a_1 of the incident wave cannot be zero or else (16) blows up. Also, if a_1 is too small relative to the incident waveform peak amplitude, a noisy solution results. These problems were solved by removing the elements a_1, a_2, \dots until a value was found that was at least 8% of the maximum value. Factors of 5% to 20% generally yielded well-behaved and accurate results.

IV. EXAMPLE

Shaped optical pulses for laser fusion experiments have been generated using the apparatus shown in Fig. 1. The configuration used was a reflecting nonuniform line driven by a 50 ps rise time step input from the Auston switch pulser. The desired electrical pulse is shown in Fig. 7, characterized by two initial pulses approximately 500 ps wide, followed by a 1.1 ns drive pulse. Notable in this pulse is the requirement that the voltage return to zero between the peaks. Layer peeling was applied to design a transmission line which would reflect this pulse shape, with $\Delta t=5$ ps and a relative dielectric constant of 1 (for the prototype line). Implemented on a VAX 8650, the computations consumed less than 20 s of CPU time to solution, which is shown in Fig. 4.

Suitable line fabrication methods at these voltages are coaxial, stripline, and microstrip. Coaxial is preferred only for its excellent range of impedances and its high voltage operation when pressurized with SF_6 . Stripline was chosen, however, because of fabrication considerations and because microstrip worked poorly in the transitions to very narrow strip widths. For fabrication, 0.125-in.-thick RT-Duroid in a stripline configuration has a "reasonable" range of impedances, $5 \Omega \leq Z \leq 180 \Omega$, with corresponding strip widths of 3 in. to 5 mils. For artwork generation, we developed a software package that converted the strip dimensions to Gerber photoplotter commands, which exposed the areas where metal was to be removed. The resultant printed circuit is shown in Fig. 5, and is the physical realization of the

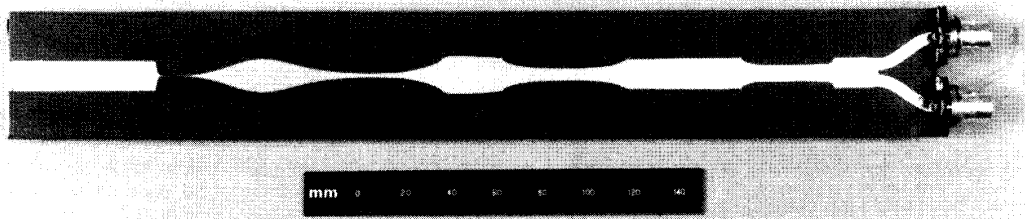


Fig. 5. Photograph of the nonuniform stripline prior to installing the cover ground plane. It was fabricated in 0.125 RT-Duroid with type C connectors.

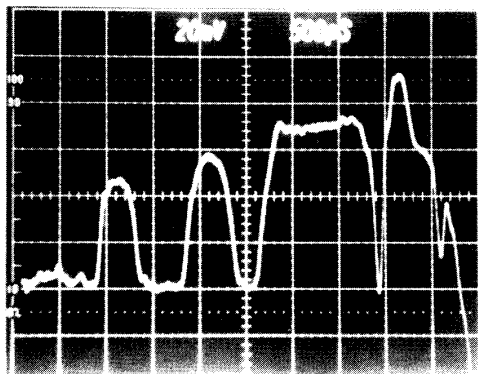


Fig. 6. Reflected waveform from the nonuniform line for an incident step excitation waveform, measured using a < 30 ps step (Tek S-52 generator) and a Tek S-6 sampling head.

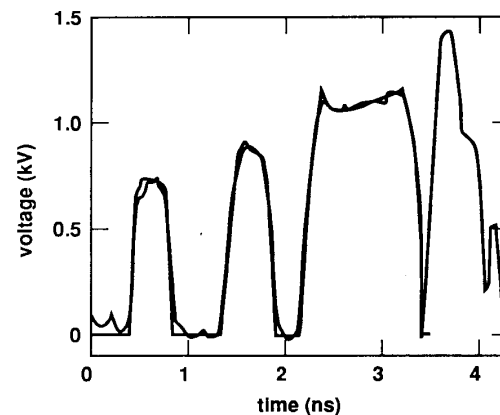


Fig. 7. The desired reflected waveform that was used in the example is overlaid with the measured result from Fig. 6. The desired waveform becomes identically zero between the peaks, and terminates at 3.5 ns. The measured waveform shows the unwanted (but irrelevant) peak which occurs after 3.5 ns.

impedance profile from Fig. 4. The strip widths were determined using Howe [17] and a zero-finding routine. For our experiments we actually fed the nonuniform line with two parallel 50Ω lines, which allowed our starting impedance to be 25Ω . The choices for high-frequency, high-voltage connectors are limited to HN, C, and SC, and we chose C because of their availability and ease of use. A panel mount C with the round center pin machined to a 10 mil flat was soldered to the strip, with the connector body then soldered to the outer ground planes.

The step response of the line was measured using a Tektronix 7104 oscilloscope with a 7S12 sampling TDR plug-in which was equipped with an S-52 pulse generator and an S-6 sampling head. The 50Ω output from the TDR was split by an unmatched SMA tee and fed through matched-length 50Ω cables to the nonuniform line. The line response is shown in Fig. 6, and is overlaid with the desired pulse shape (after amplitude scaling) in Fig. 7. The last narrow pulse following the main (wide) pulse in Fig. 7 is an artifact irrelevant to the line synthesis. This is because the desired response is specified only up to the 3.5 ns point, after which the leftover line voltage propagates out as it will. The leftover energy did not appear in the optical pulse, however, since it was sliced out by the second Pockels cell. Simulation of the impedance profile using a one-dimensional finite difference program [18] reproduced the desired waveform nearly identically, including the unwanted peak after the main

pulse. Throughout our efforts to synthesize useful lines, analysis by the finite difference method proved quite valuable as a design check. A typical simulation of 6000 time steps on a line sectioned into 900 sections of 0.5 mm required 42 s of CPU time on a VAX 8650, in double precision. Simulations were also performed on a switched charged line designed to generate the pulse shape in Fig. 7, verifying, at least computationally, the concept.

V. CONCLUSIONS

Using the layer peeling method we were able to synthesize a complex high-voltage pulse shape for use in laser fusion experiments to an extraordinary degree of precision. Furthermore it is possible to generate any arbitrary pulse shape by reflecting a step pulse off a synthesized nonuniform transmission line, provided the power spectrum of the reflected pulse does not exceed that of the input pulse at any frequency. The main disadvantage of this pulse shaping method is that the shaped pulse travels directly back at the generator, which limits the choice of pulse generators to a charged line with a series switch on both ends. In the switched charged line configuration, only one switch is required, but the voltage pulse is offset by $V_0/2$ for a matched load.

ACKNOWLEDGMENT

The authors wish to thank E. Padilla, who assembled and tested the prototypes, and W. Manchester for his help in the photo-plotter command file creation and artwork generation. Many thanks also to the Inertial Confinement Fusion Program, which was very supportive of this work.

REFERENCES

- [1] S. I. Orlov, "Concerning the theory of nonuniform transmission lines," *J. Tech. Phys. USSR*, vol. 26, p. 2361, 1956; (Transl. by American Physical Society *Sov. Phys.—Tech. Phys.*, vol. 1, pp. 2284–2294, 1957).
- [2] D. C. Youla, "Analysis and synthesis of arbitrarily terminated lossless nonuniform lines," *IEEE Trans. Circuit Theory*, vol. CT-11, pp. 363–372, Sept. 1964.
- [3] M. R. Wohlers, "A realizability theory for smooth lossless transmission lines," *IEEE Trans. Circuit Theory*, vol. CT-13, pp. 356–363, Dec. 1966.
- [4] B. Gopinath, "Inversion of the telegraph equation and the synthesis of nonuniform lines," *Proc. IEEE*, vol. 59, pp. 383–392, Mar. 1971.
- [5] A. M. Bruckstein and T. Kailath, "Inverse scattering for discrete transmission-line models," *SIAM Rev.*, vol. 29, pp. 359–389, Sept. 1987.
- [6] A. Bruckstein and T. Kailath, "An inverse scattering framework for several problems in signal processing," *IEEE ASSP Magazine*, pp. 6–20, Jan. 1987.
- [7] G. F. Ross, "The synthetic generation of phase-coherent microwave signals for transient behavior measurements," *IEEE Trans. Microwave Theory Tech.*, vol. MTT-13, pp. 704–706, Sept. 1965.
- [8] L. H. Luthjens, M. L. Hom, and M. J. W. Vermeulen, "Subnanosecond pulsing of a 3-MV Van de Graaff electron accelerator by means of a passive coaxial pulse shaper," *Rev. Sci. Instrum.*, vol. 49, pp. 230–235, Feb. 1978.
- [9] L. H. Luthjens, M. J. W. Vermeulen, and M. L. Hom, "Remotely controlled passive pulse-shaping device for subnanosecond duration voltage pulses with stepwise selectable pulse length," *Rev. Sci. Instrum.*, vol. 53, pp. 476–478, Apr. 1982.
- [10] W. Margulis and R. Persson, "Coaxial electrical pulse shaper for picosecond electronics," *Rev. Sci. Instrum.*, vol. 56, pp. 1586–1588, Aug. 1985.
- [11] W. Margulis and W. Sibbett, "Ultrafast voltage pulse shaping for streak and framing camera deflection," *Opt. Commun.*, vol. 51, pp. 91–94, 15 Aug. 1984.
- [12] M. Haner and W. S. Warren, "Generation of arbitrarily shaped picosecond optical pulses using an integrated electrooptic waveguide modulator," *Appl. Opt.*, vol. 26, pp. 3687–3694, Sept. 1987.
- [13] D. H. Auston, "Picosecond optoelectronic switching and gating in silicon," *Appl. Phys. Lett.*, vol. 26, pp. 101–103, Feb. 1975.
- [14] R. B. Wilcox, "Photoconductive switch pulse shaping device for the nova master oscillator," *Laser and Particle Beams*, vol. 4, part 1, pp. 141–143, Feb. 1986.
- [15] G. M. McWright, "Simplified theory of variable impedance stripline under pulse excitation," *Rev. Sci. Instrum.*, vol. 56, pp. 2151–2153, Nov. 1985.
- [16] R. B. Wilcox, U.S. Patent 4 667 161, May 19, 1987.
- [17] H. Howe, *Stripline Circuit Design*. Norwood, MA: Artech House, 1974, pp. 33–37.
- [18] K. S. Yee, "Numerical solution of initial boundary value problems involving Maxwell's equations in isotropic media," *IEEE Trans. Antennas Propagat.*, vol. AP-14, pp. 302–307, May 1966.

Electromagnetic Wave Transmission in a Well Logging Cable—Theory

JAMES R. WAIT, FELLOW, IEEE

Abstract—A well logging cable is idealized as a uniform cylindrical structure consisting of N axial dielectric-coated thin wires in a lossy medium, all encased by a metallic sheath. A general modal equation is developed which is specialized to low frequencies where quasi-static conditions prevail. It is pointed out that the line parameters are spa-

tially dispersive in addition to being frequency dependent. The formulation differs from most multiconductor transmission theories because of the presence of the lossy filler material, which actually allows for a simplification of the working mode equation, which is an N -order polynomial.

I. INTRODUCTION

Multiconductor cables continue to be employed for transmission of information in adverse environments. A good example is the well logging cable, which is lowered into deep boreholes. For structural reasons the cable must be supported and protected by a concentric steel sheath. The individual conductors (typically seven or eight) located in the lossy plastic filler are each coated with a dielectric of minimal loss. Because the cables have been designed from a mechanical engineering viewpoint, the electrical performance is not optimum. Nevertheless, there is a need to understand the quality of the signal transmission. We address this problem here. But first we review some of the relevant background investigations available in the open journal literature.

Pipes [1], in a generic paper, showed that the form of the classical differential equations is valid only in the case of a system of perfect conductors embedded in a perfect dielectric. That is, the system may be specified by self and mutual series impedances and shunt admittances only in the ideal case. He pointed out, however, that the slightly dissipative case could be handled by a perturbation of the loss-free solutions. This approach has often been employed in engineering calculations of multiconductor systems where the frequency dependence of the line parameters was accounted for but the spatial dispersion was ignored. That is, the dependence of the effective line parameters on the propagation constants of the modes was not considered. Soviet investigators (e.g. [2] and [3]) seem to have been the first to properly incorporate spatial dispersion in this context. Important subsequent theoretical developments by Lenahan [4] and Belevich [5] were published almost simultaneously. As they correctly point out, the general quasi-static limit is not synonymous with the TEM (transverse electromagnetic) approximation so often employed. Actually, a class of cylindrical multiconductor lines has been analyzed by a "rigorous" iterative method by Chan and Mittra [6] but it is not obvious if the spatial dispersion of the line parameters has been incorporated. Similar comments apply to the analysis by Cangellaris [7], who was concerned with excitation of the system by sources. But, for their applications, the TEM approximation may be adequate.

A key ingredient of a rigorous quasi-static analysis of a multiconductor system is to allow for the intrinsic coupling between the TE (transverse electric) and TM (transverse magnetic) field configurations in obtaining a valid mode equation before examining the low-frequency limit of the solution. A good example of a case where such an approach is needed is in the analysis of radio wave transmission in a conductor-laden tunnel [8]–[11]. In such cases, the line parameters are certainly spatially dispersive in addition to being frequency dependent. This tunnel configuration has certain similarities to the multiconductor well logging cable although there is the important distinction that, in the well logging case, the filler is a lossy dielectric.

It is our purpose here to present the relevant formulation for the well logging cable and reduce it to a form for numerical studies.

Manuscript received February 6, 1990; revised April 26, 1990.
The author is at 2210 East Waverly, Tucson, AZ 85719.
IEEE Log Number 9037687.